Metabolic and Endocrine Disorders

Giuseppe Guglielmi and Silvana Muscarella

Contents

G. Guglielmi (✉) · S. Muscarella
Department of Radiology, University of Foggia, Viale L. Pinto 1, 71100 Foggia, Italy
e-mail: g.guglielmi@unifg.it

G. Guglielmi · S. Muscarella
Department of Radiology, Hospital "Casa Sollievo della Sofferenza", Viale Cappuccini 1, 71013 San Giovanni Rotondo, Italy

Abstract

Hand and wrist are well recognized as a mirror of disease for various metabolic and endocrine pathologic conditions. Among them, osteoporosis is the most common metabolic bone disorder. It is defined as "a skeletal disease, characterized by decreased bone mineral density (BMD) and micro-architectural deterioration of bone tissue, with a consequent increase in bone fragility and susceptibility to fracture" . As a disease of the elderly, its prevalence will increase as the population ages leading to a need to intensify and optimize the diagnostic techniques for its assessment. BMD is a measurement of bone mass and a reflection of the amount of calcium in bone. Currently, the *gold standard* for measuring BMD is Dual-energy X-ray Absorptiometry (DXA).

1 Introduction

Hand and wrist are well recognized as a mirror of disease for various metabolic and endocrine pathologic conditions (Theodorou et al. 2001). Among them, osteoporosis is the most common metabolic bone disorder. It is defined as "a skeletal disease, characterized by decreased bone mineral density (BMD) and micro-architectural deterioration of bone tissue, with a consequent increase in bone fragility and susceptibility to fracture" (Anonymous 2003). As a disease of the elderly, its prevalence will increase as the population ages leading to a need to intensify and optimize the diagnostic techniques for its assessment. BMD is a measurement of bone mass

A. M. Davis et al. (eds.), *Imaging of the Hand and Wrist*, Medical Radiology. Diagnostic Imaging,
DOI: 10.1007/174_2010_127, © Springer-Verlag Berlin Heidelberg 2013

and a reflection of the amount of calcium in bone. Currently, the *gold standard* for measuring BMD is Dual-energy X-ray Absorptiometry (DXA). On the basis of the T-score (the difference between the BMD of the patient under examination and the BMD of a standard young adult population) The World Health Organization (WHO) has defined as:

- *normal* T-score values of −1.0 or higher;
- *osteopenia* T-score values of less than −1.0 but higher than −2.5;
- *osteoporosis* T-score values of −2.5 or less;
- *severe osteoporosis* T-score values of −2.5 or less with a fragility fracture (Kanis JA, on behalf of the World Health Organization Scientific Group 2007).

Osteoporotic fractures may affect any part of the skeleton except the skull. Most commonly, fractures occur in the distal forearm (Colles' fracture), thoracic and lumbar vertebrae, and proximal femur (hip fracture). Fractures usually have substantial clinical and social impact. Following a fragility fracture, significant pain, disability, and deformity can ensue, compromising life quality and shorten life expectancy (Cockerill et al. 2004; Center et al. 1999). Moreover, if fracture union is not achieved, the patient may suffer long-term disability due also to degenerative joint disease distal to the fracture and to reflex sympathetic dystrophy (Cosman 2005). A prior fracture increases the risk of future fractures (Cummings et al. 1995). Moreover, fractures are often under-recognized and patients who sustain a fragility fracture often do not receive adequate or appropriate medical treatment for the underlying osteoporosis. Given the substantial impact of osteoporosis on both patients and the medical community, it is imperative that physicians improve awareness and knowledge of osteoporosis in the setting of low-energy fractures.

2 Classification of Osteoporosis

Osteoporosis is generally characterized into primary and secondary causes. Primary osteoporosis is divided into type I, postmenopausal osteoporosis, and type II, senile or age-related osteoporosis. Type I represents a high turnover state that occurs after menopause. Type II is largely a failure of osteoblastic bone to form (Lane et al. 2006). In "postmenopausal" osteoporosis there is an apparent excess loss of cancellous bone with relative sparing of cortical bone, and the clinical syndrome involves Colle's fracture and vertebral fracture. In "senile" osteoporosis there is a more simultaneous loss of both cortical and cancellous bone. The pathogenesis of senile osteoporosis is uncertain, but it is postulated to result from an age-related decline in renal production of 1,25-dihydroxyvitamin D and calcium malabsorption, with subsequent secondary hyperparathyroidism. Fracture syndrome often seen in the patient with senile osteoporosis characteristically involves the hip and pelvis (Ross 1998). Besides the above mentioned, other risk factors like presence of dementia, susceptibility to falling, history of fractures in adulthood, history of fractures in a first-degree relative, frailty, impaired eyesight, insufficient physical activity and low body weight can partly contribute to the development of osteoporosis and its complications (Guglielmi et al. 2008).

Secondary osteoporosis is caused by a multitude of factors, including endocrine disorders, hematopoietic diseases, immobilization, gastric disorders, medications (long-term oral glucocorticoid therapy), increased alcohol intake and smoking (Seeman et al. 1983).

3 Diagnosis of Osteoporosis

3.1 Conventional Radiography

Indications of bone loss on radiographs are generally a reduction in density and changes in morphology. It has been estimated that in most cases osteopenia becomes detectable on conventional radiographs only after a loss of at least 20–40% of the skeletal bone mass (Virtama 1960; Grampp et al. 1993). Nevertheless, conventional radiography is widely available, and it remains useful for the detection of specific alterations in certain instances (e.g., subperiosteal resorption in hyperparathyroidism). Alone and in conjunction with modern, computed-aided, imaging techniques, conventional radiography is widely used for the detection of fractures, for the differential diagnosis of osteopenia, or for follow-up examinations in specific clinical settings (Genant et al. 1996; Guglielmi et al. 1994). Moreover, conventional radiographies are predominantly performed at sites of the peripheral skeleton (calcaneus and distal radius) as surrounding soft tissue does not compromise image

quality and standardization (Caligiuri et al. 1994; Vokes et al. 2006).

In osteoporosis a decrease in the mineralized bone volume results in a decrease of the total bone calcium and a decreased absorption of the X-ray beam. This phenomenon is then referred to as *increased radiolucency*. As bone mass is lost, changes in the bone structure occur. Bone is composed of two compartments: cortical bone and trabecular bone. The structural canes seen in the cortical bone represent bone resorption at different sites (e.g., the inner and outer surfaces of the cortex, or within the cortex in the Haversian and Volkmann channels). These three sites (endosteal, intracortical, and periosteal) may react differently to distinct metabolic stimuli. Cortical bone remodeling typically occurs in the endosteal "envelop", and the interpretation of subtle changes in this layer may be difficult. With increasing age there is a widening of the marrow canal due to an imbalance of endosteal bone formation and resorption that leads to a "trabeculization" of the inner surface of the cortex. Endosteal scalloping due to resorption of the inner bone surface can be seen in high-bone turnover states like reflex sympathetic dystrophy. Intracortical bone resorption may cause longitudinal striation or tunneling. These changes are seen in various high-turnover metabolic diseases affecting the bone like hyperparathyroidism, osteomalacia, renal osteodystrophy, and acute osteoporoses from disuse or reflex sympathetic dystrophy syndrome, but also rapidly evolving postmenopausal osteoporosis. It is usually not apparent in disease states with relatively low turnover like senile osteoporosis.

Accelerated endosteal and intracortical resorption, with intracortical tunneling and indistinct border of the inner cortical surface, is best depicted with high-resolution radiographic techniques with optical magnification.

Subperiosteal bone resorption is associated with an irregular definition of the outer bone surface. This finding is pronounced in diseases with high bone turn-over, principally primary and secondary hyperparathyroidism (Guglielmi et al. 2001, 2003).

In the appendicular skeleton, changes in the trabecular and cortical bone are first apparent at the ends of long and tubular bones due to the predominance of cancellous bone in these regions.

Radiologic imaging of the hand is a fundamental step in evaluating grade and type of osteoporosis, thanks to anatomic peculiarities of this anatomic region that allow a best detailed evaluation through high-resolution systems (e.g., industrial films).

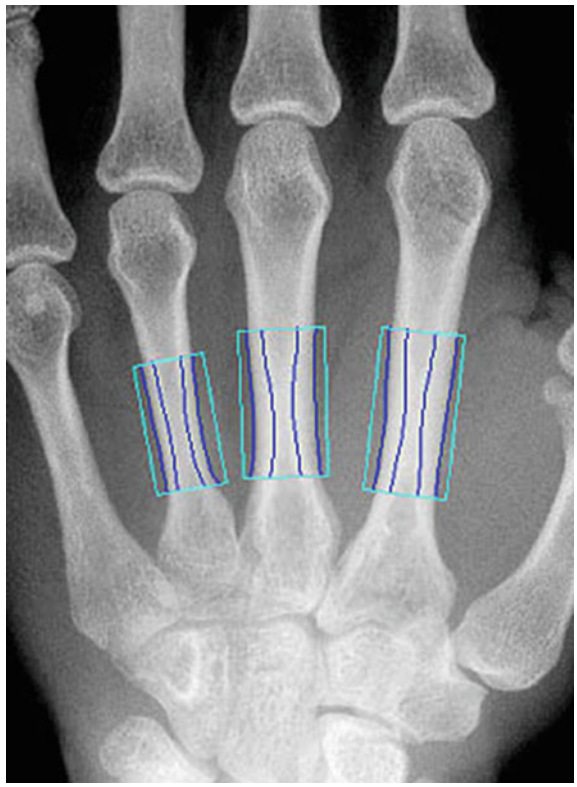

Fig. 1 Radiographs of the hand showing a detailed evaluation of II, III, and IV metacarpal bones. Spongious and cortical compartments are separately evaluated

Metacarpal bones (usually II, III, and IV) are investigated. Spongious and cortical compartments are separately evaluated (Fig. 1). The cortico-medullar index, based on the evaluation of the cortical thickness at II metacarpal bone, represented in the past a good semi-quantitative measure for grading osteoporosis at this site (Link et al. 1994).

3.2 Peripheral Dual-Energy X-Ray Absorptiometry

Bone mineral density is an important factor influencing bone strength and a key predictor of fracture risk in patients with osteoporosis and other metabolic bone diseases (Cummings et al. 2002; Grampp et al. 1997). DXA is the most widely used technique for diagnosis of osteoporosis (Cauley et al. 2005;

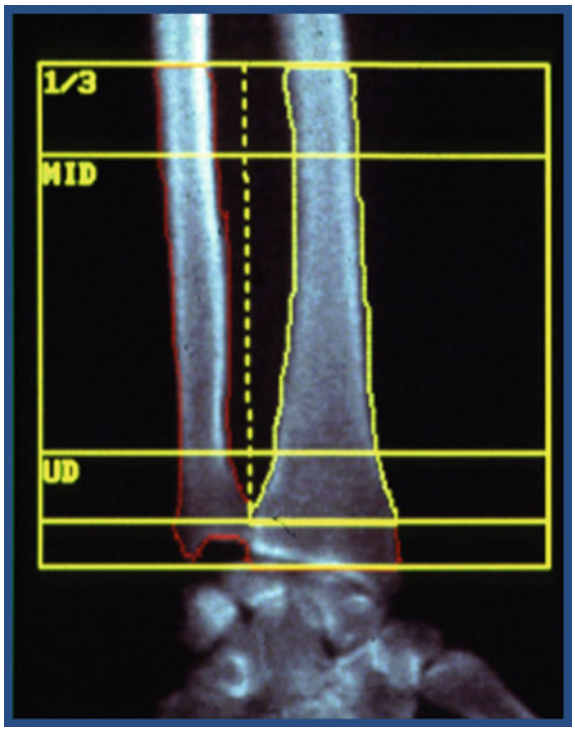

Fig. 2 DXA of the distal (87% cortical bone) and ultradistal (65% trabecular bone) forearm

Damilakis et al. 2006; Guglielmi et al. 2003). This technique determines an aerial density and BMD is therefore given as g/cm^2. It has a limited ability to evaluate bone geometry and cannot provide separate cortical and trabecular bone evaluations (Seeman and Delmas 2006).

An increasing number of small, portable DXA scanners are becoming available for application to peripheral sites (distal radius and calcaneus). Scanning of the forearm takes about 5 min to perform. The position of the forearm is standardized by the patient gripping a vertical rod. DXA allows an evaluation of weight-bearing and not weight-bearing bones. The scan is performed in a rectilinear fashion at a distal (87% cortical bone) and ultradistal (predominantly 65% trabecular bone) site (Fig. 2). Accuracy is 3%, precision is better than 1% and radiation dose is 0.1 μSv. Due to its composition, the forearm site is not a sensitive site for monitoring changes in BMD with respect to the calcaneus that is 95% trabecular bone and offers more potential for this purpose. The WHO criterion for the diagnosis of osteoporosis (T-score of −2.5 or less) is applicable to the forearm but the definitive threshold for diagnosis has still to be determined (Pacheco et al. 2002). By consequence, BMD changes in peripheral bones such as phalanx and forearm must be very carefully interpreted. In fact, screening individuals using peripheral sites and technologies is not completely supported by current evidences. Picard and collaborators (Picard et al. 2004) compared results of BMD obtained at the forearm and phalanges with those obtained at lumbar spine and femoral neck evaluated by DXA: even though the negative predictive value reached more than 95% of the true negatives, the positive predictive value was only ranged from 40 to 43% what is, again, distant from the ideal situation. In general, it is recognized that the elder the subject is, the more likely to have agreement between a peripheral and a central measurement (Deng et al. 1998).

Monitoring treatment could be a very specific applicability but, even in this case, distal sites are not completely accepted due, mainly, to the fact that the changes expected with the available therapies are also smaller than at central sites. As reviewed by the ORAG group (Guyatt et al. 2002), if the forearm was used for monitoring treatment, only the treatment with Hormonal Therapy and Alendronate for 2–4 years could be adequately monitored.

3.3 Peripheral Quantitative Computed Tomography

Bone strength and fracture risk are also influenced by parameters of bone quality such as micro-architecture and tissue properties, evaluable by developing techniques other than DXA. Peripheral Quantitative Computed Tomography (pQCT) has been proposed as a relatively inexpensive method to assess trabecular BMD in single-slice mode (Rüegsegger et al. 1976; Schneider and Börner 1991; Guglielmi and Lang 2002; Guglielmi et al. 1997). Dedicated peripheral CT scanners are available for assessing BMD in the radius and tibia. They are smaller, more mobile and less expensive that whole body CT scanners. pQCT measures the apparent volumetric BMD (mg/cm^3), in contrast to projection techniques such as DXA of the radius, and allows separate assessments of trabecular and cortical bone (Ito et al. 1997; Schneider and Reiners 1998) (Fig. 3). Peripheral QCT is most commonly applied to the non-dominant forearm.

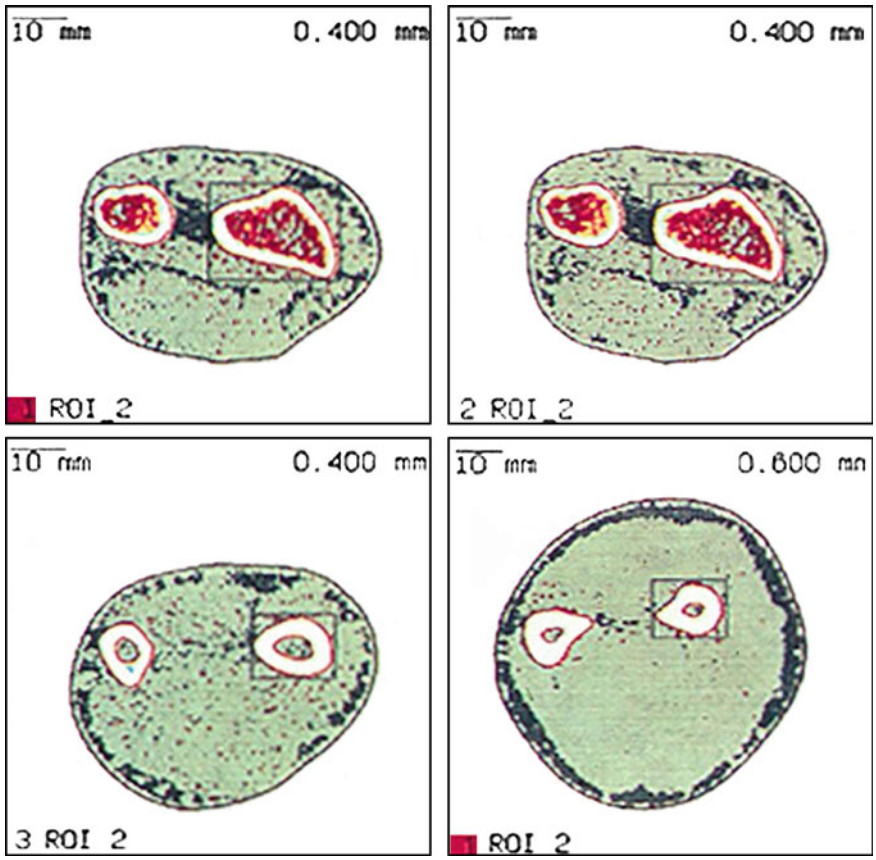

Fig. 3 Peripheral QCT of the distal radius allows separate measurement of trabecular bone, cortical bone, total and cortical area and marrow cross-sectional area

Initially the forearm length is measured as the distance between the tip of the ulnar styloid and the olecranon. The patient's forearm is placed pronated in the pQCT gantry with the elbow resting on a block and the hand gripping the hand fixture. The arm is secured with Velcro straps to prevent movement. A coronal scout scan is performed and a reference line is placed to bisect the medial border of the end of the distal radius. Accurate and consistent positioning of this reference line is essential in any longitudinal or multi-center studies for comparable results. The sites generally scanned in the radius are the 4% (distal), 50% (mid) and between 60 and 66% (proximal) shaft, but other sites (e.g., 38% distal) are also used. The parameters measured at the 4% site include total and trabecular bone mineral content (BMC), BMD and cross-sectional area (CSA); in the shaft cortical BMC and BMD are measured with many geometric parameters including total and cortical area (mm^2), cortical thickness (mm), marrow cross-sectional area (mm^2), periosteal and endosteal circumference (mm), (Adams 2009). The definition of osteoporosis given by the WHO (T-score of −2.5 or less), is applicable only to DXA of the lumbar spine, femoral neck, total hip and distal 33% radius. The definition does not apply to other anatomical sites (e.g., calcaneus) or to other densitometric techniques, such as Quantitative Ultrasound (QUS) or QCT, in either a central or peripheral QCT in the spine, and in distal radius and tibial sites.

Measurements of either total or trabecular BMD of the ultra-distal radius, by pQCT, predict fractures of the hip in post-menopausal women (Engelke et al. 2008). pQCT performs as well as, if not better than, DXA spine or QCT spine for prediction of wrist and hip fractures (Engelke et al. 2008).

Advantages of pQCT over axial QCT are that pQCT generates a lower radiation dose (1–2 μSv in pQCT compared with 50 μSv in spinal QCT), and that it provides substantially higher reproducibility (Guglielmi et al. 1997). Advantages of pQCT over DXA are high accuracy, separate measurement of

cortical and trabecular bone, and cross-sectional bone imaging to offer additional information.

Recent advancements in another novel technology, volumetric QCT (vQCT), offers three-dimensional (3D) information, and cortical and trabecular bone can be separately analyzed. A particular challenge of volumetric BMD (vBMD) is the reproducible location of a given analysis volume of interest (VOI) in longitudinal scans. Most analysis software is experimental and only a few commercial programs are available. The overall advantages of this vQCT technique include high precision, on the order of 1–2% for BMD of the spine, hip and radius; nearly instant availability of data, in a matter of seconds to minutes; widespread access, with many thousands of systems available worldwide; and minimal user interaction. The major disadvantage for vBMD is the use of modest radiation exposure, which for the radius requires an effective dose <10 μSv (Genant et al. 2008). Guglielmi et al. found that pQCT of the ultradistal radius is a precise method for measuring the true volumetric BMD and for detecting age-related bone loss in the trabecular and total bone of female subjects encompassing the adult age range and menopausal status (Guglielmi et al. 2000).

Another area of active research is high-resolution peripheral QCT (HR-pQCT), that allows accurate and precise 3D evaluation of vBMD, quantitative trabecular structure analysis of the distal radius and also a separate assessment of cortical and trabecular BMD, although with longer scan times and increased likelihood of motion artifacts (Boutroy et al. 2008; Sornay-Rendu et al. 2009). The advancement of techniques allowing assessments of cortical bone is important. Indeed, non-vertebral fractures are a significant cause of morbidity and mortality in osteoporosis, and cortical bone can account for a significant amount of the likelihood for fracture in the peripheral skeleton. On the other hand, occurrence of a forearm fracture increases the risk of future hip, spine, and forearm fractures (Cuddihy et al. 1999). This is of particular importance if one thinks that although they are accepted as a major fracture type, forearm fractures remain under-recognized and under-treated as osteoporosis-related fractures (Endres et al. 2007). Spadaro et al. (1994) evaluated the contributions of the cortical and trabecular compartments to bone strength at the radius and found that the cortical shell contributes substantially to bone strength.

The structure or spatial arrangement of bone at the macroscopic and microscopic levels is thought to provide additional, independent information on mechanical properties and may help to better predict fracture risk and assess response to drug intervention. Boutroy and colleagues (Boutroy et al. 2005) gave the first indication that peripheral trabecular structure assessment is indeed useful to differentiate women with an osteoporotic fracture history from controls better than DXA at hip or spine. Khosla and colleagues (Khosla et al. 2006a; Khosla et al. 2006b) examined age- and sex-related bone loss cross-sectionally and speculated as to the different patterns of bone loss in men and women.

3.4 Quantitative Ultrasound

Quantitative sonography methods have been introduced in recent years for the assessment of skeletal status in osteoporosis (Guglielmi et al. 2009). QUS involves generating ultrasound impulses that are transmitted (transversally or longitudinally) through the bone under study. The frequency range employed in QUS of bone lies between 200 kHz and 1.5 MHz. The ultrasound wave is produced in the form of a sinusoid impulse by special piezoelectric probes, and is detected once it has passed through the medium; there are two distinct probes, emitting and receiving, and the skeletal segment for evaluation is placed between them (Guglielmi and de Terlizzi 2009).

The first ultrasound parameters employed for characterizing bone tissue were: Speed of Sound (SoS) and Broadband Ultrasound Attenuation (BUA). More complex parameters have been developed from combination of SoS and BUA: Amplitude Dependent Speed of Sound (AD-SoS), stiffness, Quantitative Ultrasound Index (QUI) (Gluer and the International Quantitative Ultrasound Consensus Group 1997; Guglielmi et al. 2003). The technique is usually applied at the calcaneus, tibia, and phalanges, but has also been used at the patella and distal radius (Gnudi et al. 2000). The phalanx is a long bone consisting of a trabecular component and a cortical component, the principal determinant of the mechanical resistance of the bone. The phalanx is measured by QUS at the metaphyseal site,

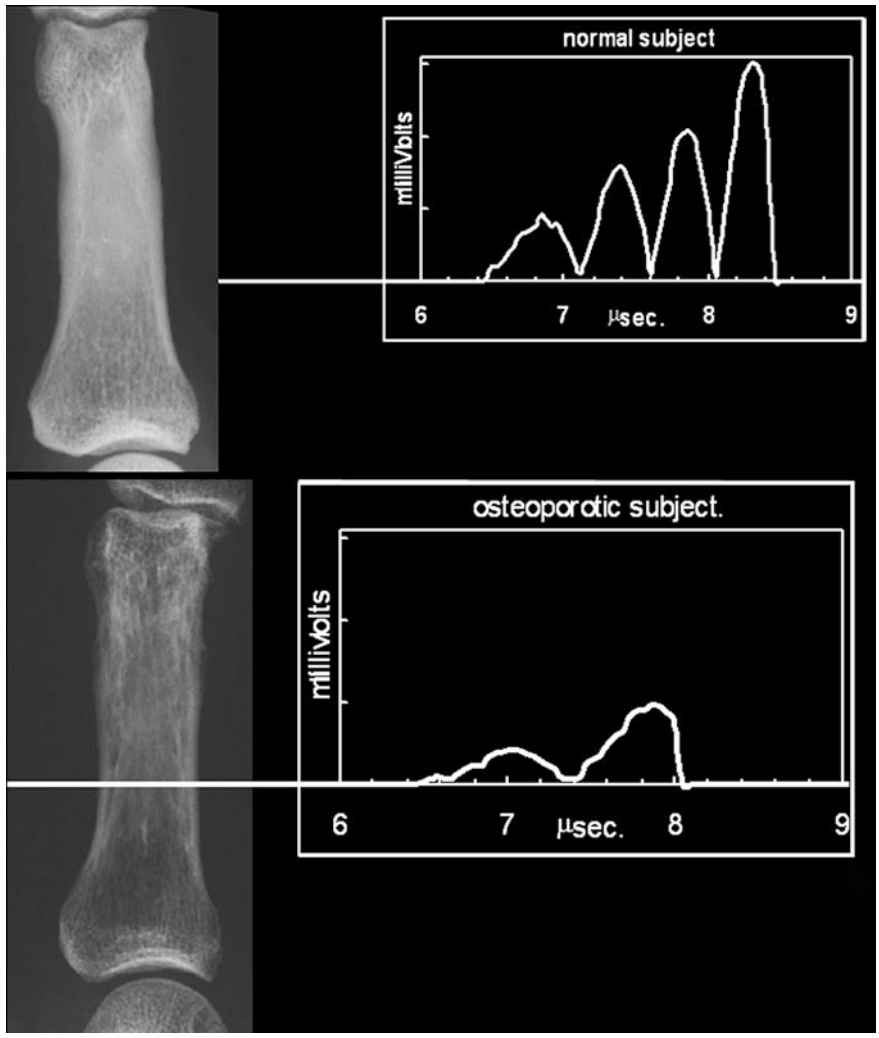

Fig. 4 Quantitative ultrasound at hand phalanges showing the different graphic traces in a normal subject and osteoporotic patient

where both trabecular (at about 40%) and cortical, bones are present. The metaphysis of the phalanx is, moreover, characterized by a high bone turnover and, therefore, extremely sensitive to changes in skeletal status due to natural causes (growth and aging), metabolic diseases (e.g., hyperparathyroidism), or drug-induced effects (treatment with glucocorticoids). When measurements are performed at the radius site, propagation occurs mainly along the external surface of the bone, and thus provides information mostly of cortical bone.

The European multi-center study (PhOS) (Wüster et al. 2000), performed on over 10.000 women, provided clinical validation of QUS at the phalanx. In this study the method could identify osteoporotic subjects with vertebral or hip fractures. Guglielmi et al. (1999) found no significant differences between phalangeal QUS and X-ray densitometric BMD methods (DXA and central QCT) in separating normal from osteoporotic subjects when using ROC analysis (Fig. 4). Hartl et al. (Hartl et al. 2002) showed that the diagnostic performance of QUS at the calcaneus and the phalanx were comparable with central DXA in assessing subjects with osteoporotic vertebral fractures. Krieg et al. (2003) studied an elderly (70–80 years) Swiss population, to assess the ability of QUS at the calcaneus and phalanx in discriminating subjects with, and without, hip fracture. An interesting Italian study demonstrated that QUS at the phalanx is more sensitive in discriminating subjects with, and without, vertebral fractures immediately post-menopause, prior to the age of

70 years, whereas QUS at the calcaneus is more sensitive in the subsequent period, at the age of 70 years and older (Camozzi et al. 2007).

Even if clinical studies demonstrated positive and statistically significant correlations between results from QUS and photon bone densitometric method, this is not sufficient to predict central BMD from QUS (Wüster et al. 2000; Guglielmi et al. 1999; Schott et al. 1995). These observations demonstrate that QUS cannot replace photon absorptiometric bone densitometry, but the two techniques can provide complementary information to improve estimates of vertebral fracture risk: low QUS values must be considered as a factor in fracture risk assessment which is independent of BMD and, therefore, emphasizes the clinical importance of QUS in appropriate clinical situations. Anyway, it is important to note that the WHO definition of osteoporosis based on densitometry terms (T-score of −2.5 or less) is not applicable to QUS. On the other hand, QUS for the study of post-menopausal osteoporosis is now completely validated: scientific societies of several European countries have included bone QUS in their national guidelines for the diagnosis and management of osteoporosis, particularly for the evaluation of fracture risk in post-menopausal women (National Osteoporosis Society 2002; Schattauer GmbH 2006). Ultrasound velocity has also been applied to monitor changes and response to treatment in women with osteoporosis. In particular, some studies show that treatment with alendronate (Ingle et al. 2005), raloxifene (Agostinelli and de Terlizzi 2007), and teriparatide (Gonnelli et al. 2006) can be monitored using phalanx QUS.

3.5 Magnetic Resonance

Magnetic resonance (MR) offers alternative ways of assessing skeletal properties. Trabecular bone is not visualized at MR imaging so that a trabecula appears as a signal void, surrounded by high-intensity fatty bone marrow. This signal void is due to the very short T2 relaxation time of bone and to the bone marrow interface (Link et al. 1999; Guglielmi et al. 2003). Due to technical advances, like optimized coil design, fast gradients and high field strength, clinical MR scanners provide an in vivo spatial resolution close to the diameter of a single trabecula (Sell et al. 2005; Wehrli 2007). Moreover, with the advent of parallel imaging, motion correction techniques and new sequences, the limits of spatial resolution and scan time can be further overcome (Banerjee et al. 2006; Techawiboonwong et al. 2005). Most in vivo studies focused on peripheral skeleton because the distal radius, distal tibia and the calcaneus are easily accessible with small coils, contain a high number of trabeculae and the bone marrow consists of fat, resulting in high bone–bone marrow contrast. Each stage needs to be standardized to ensure a high degree of reproducibility (Newitt et al. 2002). On the other hand, the processing of high-resolution MR (HR–MR) images generally consists of several stages (registration, segmentation, resolution enhancement and normalization or binarization), before measures of the trabecular architecture can be evaluated (Wehrli 2007; Newitt et al. 2002) (Fig. 5). The efficiency of these techniques was evaluated in terms of reproducibility (2–4%), (Gomberg et al. 2004) and different approaches have been applied successfully in several cross-sectional, and recently in longitudinal, studies (Wehrli et al. 2001; Majumdar et al. 1999; Cortet et al. 2000). MR imaging aims to quantification of the trabecular bone architecture trough five types of measures (describing scale; shape and orientation of the trabeculae; connectivity or complexity of the trabecular network and finite element models—FEM) directly characterizing mechanical properties.

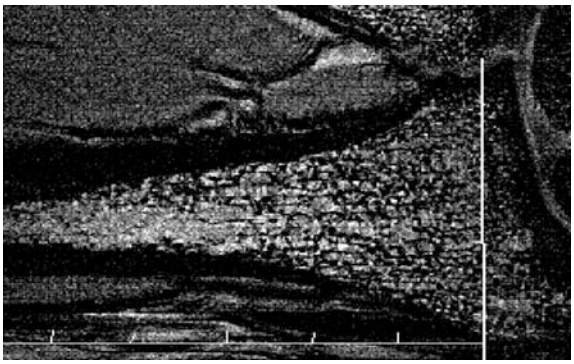

Fig. 5 High-resolution MR of the radius allows quantification of the trabecular bone architecture (scale, shape, orientation, connectivity and finite element models of the trabeculae)

Many Authors studied performances of MR in studying trabecular structure at distal radius and phalanges. Stampa et al. (2002) used phalanges, a convenient anatomic site particularly suitable for

obtaining high signal-to-noise and high-spatial resolution images, to derive quantitative three-dimensional parameters based on an algorithm and model for defining trabecular rods and plates. To date the quantification of trabecular bone architecture by HR–MR imaging at distal radius aimed to assess the prevalence and incidence of osteoporotic fractures (Majumdar et al. 1999; Cortet et al. 2000; Majumdar et al. 1997). Early studies suggested that MR-based parameters of the trabecular architecture better separate patients with, and without, osteoporotic fractures compared to BMD (Cortet et al. 2000; Majumdar et al. 1997). Link et al. (1998), Majumdar et al. (Majumdar et al. 1997), and Wehrli et al. (Wehrli et al. 1998; Wehrli et al. 2001; Wehrli et al. 2002) have shown the ability to discriminate spine and/or hip fractures using trabecular structure or textural parameters from in vivo MR images of the radius. In measuring the effect of pharmacological therapies for osteoporosis, some studies shows that parameters of trabecular micro-architecture derived by MR could better monitor changes due to anti-resorptive treatment than BMD (Chesnut et al. 2005). One of the early longitudinal studies showed that salmon calcitonin had therapeutic benefit compared with placebo in maintaining trabecular micro-architecture at multiple skeletal sites (Chesnut et al. 2005).

4 Other Metabolic and Endocrine Disorders

4.1 Acromegaly and Gigantism

These conditions are characterized by excess production of growth hormone (GH) due to acidophilic adenomas of the anterior lobe of the pituitary gland or from diffuse hyperplasia of the acidofilic cells. GH excess, which can arise in children (gigantism) or in adult (acromegaly), leads to an overgrowth of bone in the skeleton. In the immature skeleton the disease is associated with extreme height and a large skeleton with normal bone age. In the mature skeleton, after physeal closure, excessive GH production causes an increase in width of bone and soft tissue enlargement manifested particularly in the acral parts of the skeleton.

Fig. 6 Acromegaly showing bony overgrowth, joint widening, metacarpal hooking, and arrow-head terminal tufts

Radiographic manifestations of the hand in patients with acromegaly include soft tissue thickening of the digits, osseous enlargement and increased width by means of thickening and squaring of the phalanges and metacarpal bones, overconstrictions or overtubulation of the shafts of the phalanges with normal or increased cortical thickness, widening of the articular spaces due to thickening of the articular cartilage, bone proliferation at tendon and ligament attachment site (enthesopathy) (Fig. 6).

In diagnosing early acromegalic changes some indexes have been proposed. Among them the sesamoid index, proposed by Kleinberg et al. (1966). According to this method, the size of the medial sesamoid at the first metacarpophalangeal joint is measured. This index has, however, a limited reliability because of the significant overlap in measurements in acromegalic patients and controls. Besides bone proliferation, bone resorption can associate (Resnick 1995), leading to a decreased bone density, particularly in the late stages of disease (Sartoris 1971). In addition, osteoarthritis usually complicates the disease (Resnick 1995).

4.2 Hypopituitarism

Hypopituitarism can arise from many causative factors (neoplasms, surgery, irradiation, injury, vascular insult, infection, and granulomas of the pituitary gland or the hypothalamus). Familial pituitary deficiency is reported in 10% cases. Isolated GH deficiency during the period of skeletal growth leads to abnormality of osseous development as a delay in appearance and growth of ossification centers and a similar delay in their fusion and disappearance (Resnick 1995). Radiographic manifestations in the hand include shortening and broadening of the metacarpal bones and distal phalanges or, less commonly, a hypoplastic appearance of the distal phalanges, metaphyseal irregularity, flattening and absence of closure of the physes, and severe osteoporosis. Open epiphyses may be observed in the distal portions of the radius and ulna (Resnick 1995).

4.3 Thyroid Disorders

Thyroid hormone increases bone remodeling (Mosekilde et al. 1990). In cases of excessive thyroid hormone, osteoclastic activity predominates on osteoblastic one, with resultant bone resorption. In the hand, hyperthyroid osteopathy leads to bone loss that is manifested as a lattice-like appearance in the phalanges, and "flaky" cortices due to radiolucent intracortical striations (Resnick 1995). In hypothyroidism, bone abnormalities are more evident in neonates, children, and young adults, and result in retardation of skeletal maturation with subsequent retardation in growth. Delayed appearance and growth of epiphyseal ossification centers, and abnormality of physeal development accompanied by delayed physeal closure are observed. In the hand, arrest in growth is manifested as shortening and widening of the metacarpal bones, which present endosteal cortical thickening (Fig. 7) (Steinbach et al. 1975). Hypoplastic phalanges of fifth finger may be seen (Sartoris 1996). In affected epiphyses, ossification proceeds from multiple centers rather than from a single site (pseudoepiphyses). Abnormal epiphiseal ossification results in a characteristic irregular ad fragmented epiphyseal appearance recognized as epiphyseal dysgenesis (Borg et al. 1975; Parker 1981).

Fig. 7 Hypothyroidism (cretinism) in a child. There is retarded skeletal maturation with shortening of the metacarpals and squaring of the epiphyses

4.4 Hyperparathyroidism

Hyperparathyroidism, a clinical condition characterized by an elevation of serum parathyroid hormone concentration, may be primary, secondary, or tertiary. In primary hyperparathyroidism, hypersecretion of parathyroid hormone is due to abnormality in the parathyroid glands (single or multiple adenomas, diffuse hyperplasia, and carcinoma). Secondary hyperparathyroidism usually is secondary to chronic renal disease, or occasionally, malabsorption states. Tertiary hyperparathyroidism occurs in patients with chronic renal disease and secondary hyperparathyroidism who develop autonomous parathyroid function.

The hand is almost always involved in hyperparathyroidism. Subperiosteal bone resorption is most frequently observed along the radial aspect of the phalanges, particularly in the middle phalanges of the index and middle fingers (Fig. 8) (Resnick 1995).

Fig. 8 Hyperparathyroidism. There is subperiosteal resorption along the middle phalanges with terminal phalangeal resorption (acro-osteolysis)

Fig. 9 Secondary hyperparathyroidism in an adult with chronic renal disease. **a** There is subperiosteal resorption along the phalanges, terminal phalangeal resorption with soft tissue and vascular calcification. **b** After successful renal transplantation the resorption has resolved as has the soft tissue but not the vascular calcification. The terminal phalanges remain stunted

Subperioteal bone resorption involves the phalangeal tufts as well, where loss of the cortical "white line" represents the earliest sign of the disease progressing to acro-osteolysis (Sundaram et al. 1979). Intracortical resorption always associates (Meema and Meema 1972) leading to development of pseudoperiostitis (Resnick 1995). Owing to rapid or severe bone loss multiple intracortical, radiolucent areas, in the form of linear striations or tunneling, may be observed in the metacarpal bone and appear more evident in the cortex of the second metacarpal bone (Meema and Meema 1972). In the hand, osteoclastic resorption occurs along the endosteal surface of bone causing localized scalloped or pocket-like defects along the endosteal margin of the cortex. In children with primary or secondary hyperparathyroidism, irregular radiolucent areas may be apparent in the metaphysis adjacent to the growth plate of tubular bones of the hand (Resnick 1995). In the hyperparathyroid state, osseous resorption may occur at sites of tendon and ligament attachment to bone also at the hand and the wrist (Resnick 1995). Trabecular resorption within medullary bone, particularly in the advanced stages of the disease, may involve the tubular bones of the hand that assume a characteristic granular appearance, with loss of distinct trabecular detail, and subsequent osseous deformities that may simulate the changes of osteomalacia (Resnick 1995). Brown tumors are also included among the radiographic manifestations of hyperparathyroidism and represent localized accumulations of osteoclasts, fibrous tissue, and giant cells, which can replace bone and occasionally produce osseous expansion. They appear as single or multiple well or poorly demarcated osteolytic lesions with an eccentric or cortical location (Resnick 1995). A prominent radiographic feature of hyperparathyroidism is generalized osteopenia. Nevertheless, as hyperparathyroidism may induce either bone resorption or formation, increased radiodensity of bones may become a prominent radiographic feature. There is a meaningful association between primary hyperparathyroidism and CPPD crystal deposition that may lead to the pseudogout syndrome. Renal osteodystrophy is the clinical term indicating bone disease in patients with chronic renal failure. The radiographic manifestations of renal osteodystrophy reflect hyperparathyroidism and deficiency of 1,25-dihydroxyvitamin D, rickets and osteomalacia, osteoporosis, soft tissue and vascular calcifications, and miscellaneous changes (Fig. 9) (gout arthritis due to hyperuricemia). Lytic, expansile lesions, the so-called brown tumor may occur in the long bones of the hand and will

mimic a giant cell tumor both radiographically and histologically (Fig. 10). They are commoner in patients with chronic renal disease because of the larger numbers of patients surviving on dialysis and that most cases of primary hyperparathyroidism are now detected on serum biochemistry.

4.5 Rickets and Osteomalacia

The terms rickets and osteomalacia refer to the same condition manifesting in the child and adult, respectively. The commonest cause worldwide is inadequate dietary intake of vitamin D. Other causes include inadequate sunshine, malabsorption states, anti-epileptic drug therapy, renal disease and rarely tumur related. This results in inadequate or delayed mineralization of osteoid in mature cortical and spongy bone (osteomalacia) and from an interruption in orderly development and mineralization of the growth plate (rickets) (Resnick 1995). As rachitic changes are more evident in regions of the most active bone growth, target sites of rickets include the distal ends of ulna and radius (Park 1932). General radiographic features of rickets include retardation in bone growth and osteopenia. Slight axial widening of the physis represents the earliest specific radiographic finding (Steinbach and Noetzli 1964). Disorganization and "fraying" of the spongy bone occur in the metaphyseal region, which eventually demonstrates widening and cupping (Fig. 11) (Resnick 1995). In the hand of the rachitic children, irregularities and widening of the physes seen in the metacarpals and phalanges also may be associated with bone resorption. In osteomalacia medullary bone shows a decrease in the total number of trabeculae, owing to a loss of secondary trabeculae. The remaining bone trabeculae are prominent and present a "coarsened" pattern with unsharp margins reflecting deposition of inadequately mineralized osteoid. Looser's zones, typical of osteomalacia elsewhere in the skeleton, are uncommon in the hands.

4.6 Hypoparathyroidism

Hypoparathyroidism is a general term describing a clinical state of parathyroid hormone deficiency, which results in hypocalcemia and neuromuscular

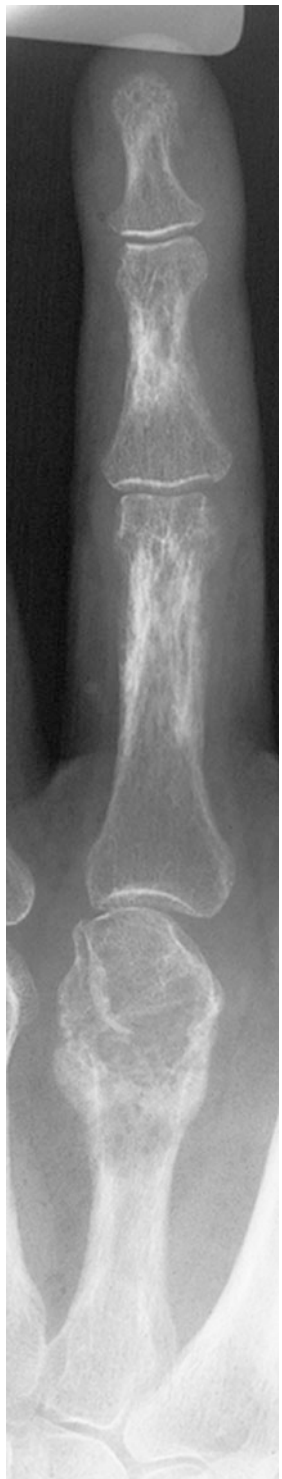

Fig. 10 Brown tumor in a patient with chronic renal disease. There is a pathological fracture developing through a lytic expansile lesion in the distal end of the metacarpal. There are features of hyperparathyroidism affecting the phalanges

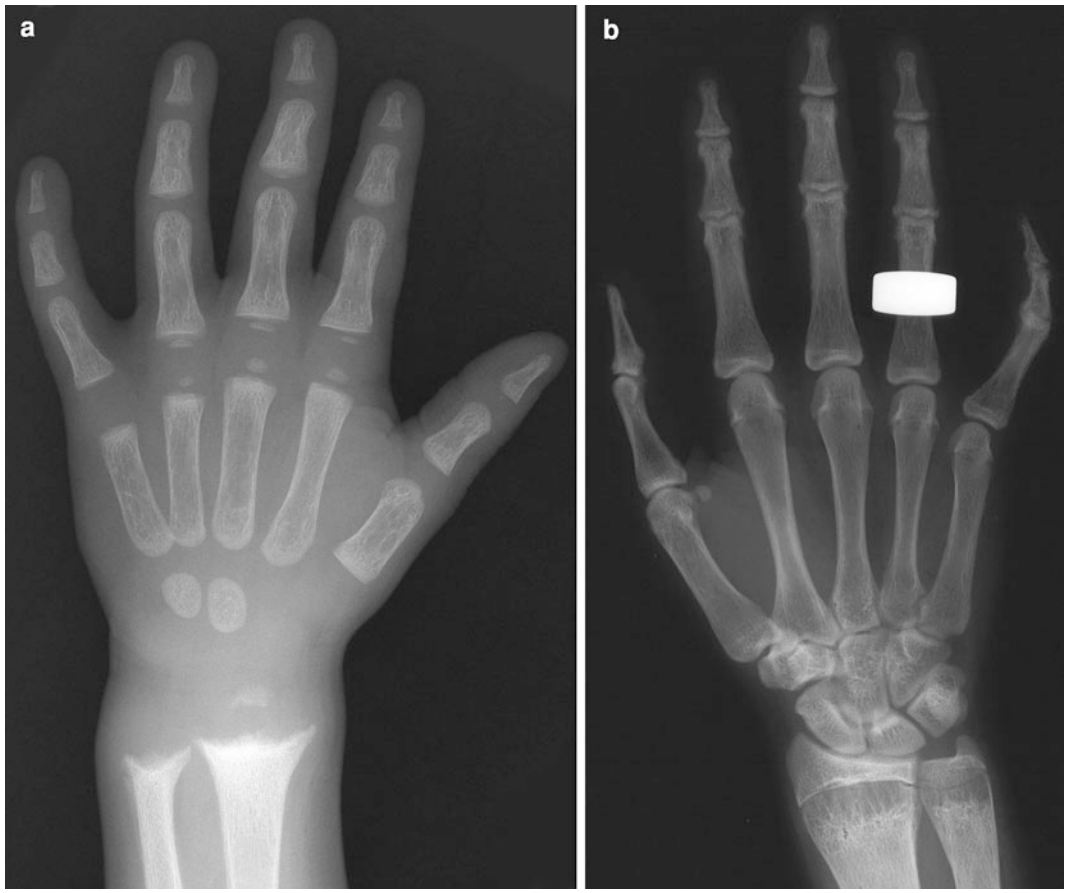

Fig. 11 Rickets. **a** In a young child there is generalized osteopenia with cupping, splaying, and fraying of the distal radial and ulnar metaphyses. **b** In an adolescent the only abnormalities are generalized osteopenia and relative demineralization of the distal radial and ulnar metaphyses

dysfunction. It can have many causes like surgery, congenital absence or atrophy of the parathyroid glands, and parathyroid gland destruction after radiation. The major radiographic manifestations of hypoparathyroidism are osteosclerosis, which may be generalized or localized, and soft tissue calcification. In the hand, radiographic findings of hypoparathyroidism are usually subtle and represented by subcutaneous, ligamentous and tendinous calcifications, premature fusion of the physes, entsopathy, and osteoporosis (Resnick 1995).

Pseudohypoparathyroidism (PHP) or Albright's hereditary osteodystrophy, is a congenital disorder characterized by hypocalcemia and hyperphosphatemia. Pseudopseudohypoparathyroidism (PPHP) is the normocalcemic form of PHP and is also caused by failure and end-organ response to parathyroid hormone. In the hand, radiographic findings of PHP and PPHT include shortening of the metacarpal bone and phalanges secondary to premature physeal closure, widening and shortening of the phalanges with presence of cone-shaped and pseudo-epiphyses, soft tissue calcification, and small diaphyseal exostoses that extend perpendicularly from the surface of the bone (Fig. 12). In most cases of PHP and PPHP, metacarpal shortening shows predilection for the first, fourth, and fifth rays and may lead to a positive metacarpal sign (the line drawn tangential to the heads of the fourth and fifth metacarpal bones intersects the end of the third metacarpal bone, indicating disproportionate shortening of the fourth and fifth metacarpal bones).

Fig. 12 Pseudohypoparathyroidism. There is shortening of the metacarpals with soft tissue calcifications

4.7 Scurvy

Scurvy is due to a deficiency, typically dietary, of vitamin C (ascorbic acid) which leads do a reduction in collagen formation in bone. The radiographic features include generalized osteopenia, thinned cortices with sparse trabeculae, dense metaphyseal line with an adjacent lucent line, metaphyseal spurs (Pelkan spurs) and finely pencilled dense epiphyseal margins (Wimburger's sign). Capillary fragility may lead to subperiosteal hemorrhage that in time may heal with exuberant periosteal ossification. All these features are more commonly seen in the lower limbs than the hand or wrist.

5 Conclusions

Several metabolic and endocrine disorders cause skeletal involving of hand and wrist. Among them osteoporosis is the most common metabolic bone disease. Besides traditional methods (conventional radiographs), new interesting techniques are developing and appear promising in the evaluation of peripheral osteoporosis. Many studies evaluate DXA application at distal radius; pQCT demonstrates promising results in studying bone microarchitecture thanks to new technologies like vQCT and HR-QCT; QUS are proving to be very useful in the evaluation of bone properties and showed good performances with respect to DXA; finally, HR-MR, on the basis of sophisticated software, is becoming a new challenging technique in the assessment of trabecular structure. Other metabolic and endocrine conditions may manifest with radiographic abnormalities in the hands including rickets and hyperparathyroidism.

6 Key Points

- Osteoporosis and other several metabolic and endocrine disorders cause skeletal involving of hand and wrist.
- DXA is the *gold standard* for measuring BMD in the axial skeleton, as defined by WHO.
- pDXA as well as pQCT are the methods of choice in the evaluation of peripheral osteoporosis.
- QUS is a useful tool in the evaluation of bone properties.
- vQCT, HR-QCT, and HR-MR, on the basis of sophisticated software, are challenging techniques in the assessment of trabecular structure.

References

Adams JE (2009) Quantitative computed tomography. Eur J Radiol 71:415–424

Agostinelli D, de Terlizzi F (2007) QUS in monitoring raloxifene and estrogen-progestogens: a 4-year longitudinal study. Ultrasound Med Biol 33:1184–1190

Anonymous (2003) Prevention and management of osteoporosis. World Health Organ Tech Rep Ser 921:1–164

Banerjee S, Choudhury S, Han ET, Brau AC, Morze CV, Vigneron DB, Majumdar S (2006) Autocalibrating parallel imaging of in vivo trabecular bone microarchitecture at 3 Tesla. Magn Reson Med 56:1075–1084

Borg SA, Fitzer PM, Young LW (1975) Roentgenologic aspects of adult cretinism. Two case reports and review of the literature. Am J Roentgenol Radium Ther Nucl Med 123:820–828

Boutroy S, Bouxsein ML, Munoz F, Delmas PD (2005) In vivo assessment of trabecular bone microarchitecture by high-resolution peripheral quantitative computed tomography. J Clin Endocrinol Metab 90:6508–6515

Boutroy S, Van Rietbergen B, Sornay-Rendu E, Munoz F, Bouxsein ML, Delmas PD (2008) Finite element analysis based on in vivo HR-pQCT images of the distal radius is associated with wrist fracture in postmenopausal women. J Bone Miner Res 23:392–399

Caligiuri P, Giger ML, Favus M (1994) Multifractal radiographic analysis of osteoporosis. Med Phys 21:503–508

Camozzi V, De Terlizzi F, Zangari M, Luisetto G (2007) Quantitative bone ultrasound at phalanges and calcaneus in osteoporotic postmenopausal women: influence of age and measurement site. Ultrasound Med Biol 33:1039–1045

Cauley JA, Lui LY, Ensrud KE, Zmuda JM, Stone KL, Hochberg MC, Cummings SR (2005) Bone mineral density and the risk of incident nonspinal fractures in black and white women. JAMA 293:2102–2108

Center JR, Nguyen TV, Schneider D, Sambrook PN, Eisman JA (1999) Mortality after all major types of osteoporotic fracture in men and women: an observational study. Lancet 353:878–882

Chesnut CH 3rd, Majumdar S, Newitt DC, Shields A, Van Pelt J, Laschansky E, Azria M, Kriegman A, Olson M, Eriksen EF, Mindeholm L (2005) Effects of salmon calcitonin on trabecular microarchitecture as determined by magnetic resonance imaging: results from the QUEST study. J Bone Miner Res 20:1548–1561

Cockerill W, Lunt M, Silman AJ, Cooper C, Lips P, Bhalla AK, Cannata JB, Eastell R, Felsenberg D, Gennari C, Johnell O, Kanis JA, Kiss C, Masaryk P, Naves M, Poor G, Raspe H, Reid DM, Reeve J, Stepan J, Todd C, Woolf AD, O'Neill TW (2004) Health-related quality of life and radiographic vertebral fracture. Osteoporos Int 15:113–119

Cortet B, Boutry N, Dubois P, Bourel P, Cotten A, Marchandise X (2000) In vivo comparison between computed tomography and magnetic resonance image analysis of the distal radius in the assessment of osteoporosis. J Clin Densitom 3:15–26

Cosman F (2005) The prevention and treatment of osteoporosis: a review. MedGenMed 7:73

Cuddihy MT, Gabriel SE, Crowson CS, O'Fallon WM, Melton LJ 3rd (1999) Forearm fractures as predictors of subsequent osteoporotic fractures. Osteoporos Int 9:469–475

Cummings SR, Nevitt MC, Browner WS, Stone K, Fox KM, Ensrud KE, Cauley J, Black D, Vogt TM (1995) Risk factors for hip fracture in white women. Study of Osteoporotic Fractures Research Group. N Engl J Med 332:767–773

Cummings SR, Bates D, Black DM (2002) Clinical use of bone densitometry: scientific review. JAMA 288:1889–1897

Damilakis J, Maris TG, Karantanas AH (2006) An update on the assessment of osteoporosis using radiologic techniques. Eur Radiol 17:1591–1602

Deng HW, Li JL, Li J, Davies KM, Recker RR (1998) Heterogeneity of bone mineral density across skeletal sites and its clinical implications. J Clin Densitom 1:339–353

Endres HG, Dasch B, Maier C, Lungenhausen M, Smektala R, Trampisch HJ, Pientka L (2007) Diagnosis and treatment of osteoporosis in postmenopausal women with distal radius fracture in Germany. Curr Med Res Opin 23:2171–2181

Engelke K, Adams JE, Armbrecht G, Augat P, Bogado CE, Bouxsein ML, Felsenberg D, Ito M, Prevrhal S, Hans DB, Lewiecki EM (2008) Clinical use of quantitative computed tomography and peripheral quantitative computed tomography in the management of osteoporosis in adults: the 2007 ISCD Official Positions. J Clin Densitom 11:123–162

Genant HK, Engelke K, Fuerst T, Glüer CC, Grampp S, Harris ST, Jergas M, Lang T, Lu Y, Majumdar S, Mathur A, Takada M (1996) Noninvasive assessment of bone mineral and structure: state of the art. J Bone Miner Res 11:707–730

Genant HK, Engelke K, Prevrhal S (2008) Advanced CT bone imaging in osteoporosis. Rheumatology 47:iv9–iv16

Gluer CC, The International Quantitative Ultrasound Consensus Group (1997) Quantitative ultrasound techniques for the assessment of osteoporosis: expert agreement on current status. J Bone Miner Res 12:1280–1288

Gnudi S, Ripamonti C, Malavolta N (2000) Quantitative ultrasound and bone densitometry to evaluate the risk of nonspine fractures: a prospective study. Osteoporos Int 11:518–523

Gomberg BR, Wehrli FW, Vasilić B, Weening RH, Saha PK, Song HK, Wright AC (2004) Reproducibility and error sources of micro-MRI-based trabecular bone structural parameters of the distal radius and tibia. Bone 35:266–276

Gonnelli S, Martini G, Caffarelli C, Salvadori S, Cadirni A, Montagnani A, Nuti R (2006) Teriparatide's effects on quantitative ultrasound parameters and bone density in women with established osteoporosis. Osteoporos Int 17:1524–1531

Grampp S, Jergas M, Glüer CC, Lang P, Brastow P, Genant HK (1993) Radiologic diagnosis of osteoporosis. Current methods and perspectives. Radiol Clin North Am 31:1133–1145

Grampp S, Genant HK, Mathur A, Lang P, Jergas M, Takada M, Glüer CC, Lu Y, Chavez M (1997) Comparisons of noninvasive bone mineral measurements in assessing age-related loss, fracture discrimination, and diagnostic classification. J Bone Miner Res 12:697–711

Guglielmi G, de Terlizzi F (2009) Quantitative ultrasound in the assessment of osteoporosis. Eur J Radiol 71:425–431

Guglielmi G, Lang TF (2002) Quantitative computed tomography. Semin Musculoskelet Radiol 6:219–227

Guglielmi G, Genant HK, Pacifici R, Giannatempo GM, Cammisa M (1994) The imaging diagnosis of osteoporosis. The state of the art and outlook. Radiol Med 88:535–546

Guglielmi G, Schneider P, Lang TF, Giannatempo GM, Cammisa M, Genant HK (1997a) Quantitative computed tomography at the axial and peripheral skeleton. Eur Radiol 7:32–42

Guglielmi G, Cammisa M, De Serio A, Giannatempo GM, Bagni B, Orlandi G, Russo CR (1997b) Long-term in vitro precision of single slice peripheral Quantitative Computed Tomography (pQCT): multicenter comparison. Technol Health Care 5:375–381

Guglielmi G, Cammisa M, De Serio A, Scillitani A, Chiodini I, Carnevale V, Fusilli S (1999) Phalangeal US velocity discriminates between normal and vertebrally fractured subjects. Eur Radiol 9:1632–1637

Guglielmi G, De Serio A, Fusilli S, Scillitani A, Chiodini I, Torlontano M, Cammisa M (2000) Age-related changes assessed by peripheral QCT in healthy Italian women. Eur Radiol 10:609–614

Guglielmi G, Cammisa M, De Serio A (2001) Bone densitometry and osteoporosis at the hand and wrist. In: Gulglielmi G, Van Kuijk C, Genant HK (eds) Fundamentals of hand and wrist imaging. Springer-Verlag, Heidelberg, pp 233–235

Guglielmi G, Perta A, Cammisa M (2003a) Plain radiographs in the study of osteoporotic syndrome. Radiol Med 105:1–5

Guglielmi G, Perta A, Palladino D, Crisetti N, Mischitelli F, Cammisa M (2003b) Bone densitometry in the diagnosis and follow-up of osteoporosis. Radiol Med 106:29–35

Guglielmi G, Crisetti N, Mischitelli F, Cammisa M (2003c) Quantitative ultrasound. Radiol Med 105:27–33

Guglielmi G, Toffanin R, Cova M, Cammisa M (2003d) Quantitative magnetic resonance of trabecular bone. Radiol Med 105:34–40

Guglielmi G, Muscarella S, Leone A, Peh WC (2008) Imaging of metabolic bone diseases. Radiol Clin North Am 46: 735–754

Guglielmi G, Adams J, Link TM (2009) Quantitative ultrasound in the assessment of skeletal status. Eur Radiol 19:1837–1848

Guyatt GH, Cranney A, Griffith L, Walter S, Krolicki N, Favus M, Rosen C (2002) Summary of meta-analyses of therapies for postmenopausal osteoporosis and the relationship between bone density and fractures. Endocrinol Metab Clin North Am 31:659–679

Hartl F, Tyndall A, Kraenzlin M, Bachmeier C, Gückel C, Senn U, Hans D, Theiler R (2002) Discriminatory ability of quantitative ultrasound parameters and bone mineral density in a population-based sample of postmenopausal women with vertebral fractures: results of the Basel Osteoporosis Study. J Bone Miner Res 17:321–330

Ingle BM, Machado AB, Pereda CA, Eastell R (2005) Monitoring alendronate and estradiol therapy with quantitative ultrasound and bone mineral density. J Clin Densitom 8:278–286

Ito M, Tsurusaki K, Hayashi K (1997) Peripheral QCT for the diagnosis of osteoporosis. Osteoporos Int 7:S120–S127

Kanis JA, on behalf of the World Health Organization Scientific Group (2007) Assessment of osteoporosis at the primary health-care level. Technical Report. World Health Organization Collaborating Centre for Metabolic Bone Diseases, University of Sheffield, UK, 2008

Khosla S, Riggs BL, Atkinson EJ, Oberg AL, McDaniel LJ, Holets M, Peterson JM, Melton LJ 3rd (2006a) Effects of sex and age on bone microstructure at the ultradistal radius: a population-based noninvasive in vivo assessment. J Bone Miner Res 21:124–131

Khosla S, Melton LJ 3rd, Achenbach SJ, Oberg AL, Riggs BL (2006b) Hormonal and biochemical determinants of trabecular microstructure at the ultradistal radius in women and men. J Clin Endocrinol Metab 91:885–891

Kleinberg DL, Young IS, Kupperman HS (1966) The sesamoid index. An aid in the diagnosis of acromegaly. Ann Intern Med 64:1075–1078

Krieg MA, Cornuz J, Ruffieux C, Sandini L, Büche D, Dambacher MA, Hartl F, Häuselmann HJ, Kraenzlin M, Lippuner K, Neff M, Pancaldi P, Rizzoli R, Tanzi F, Theiler R, Tyndall A, Wimpfheimer K, Burckhardt P (2003) Comparison of three bone ultrasounds for the discrimination of subjects with and without osteoporotic fractures among 7562 elderly women. J Bone Miner Res 18:1261–1266

Lane JM, Serota AC, Raphael B (2006) Osteoporosis: differences and similarities in male and female patients. Orthop Clin North Am 37:601–609

Link TM, Rummeny EJ, Lenzen H, Reuter I, Roos N, Peters PE (1994) Artificial bone erosions: detection with magnification radiography versus conventional high resolution radiography. Radiology 192:861–864

Link TM, Majumdar S, Augat P, Lin JC, Newitt D, Lu Y, Lane NE, Genant HK (1998) In vivo high resolution MRI of the calcaneus: differences in trabecular structure in osteoporosis patients. J Bone Miner Res 13:1175–1182

Link TM, Majumdar S, Grampp S, Guglielmi G, van Kuijk C, Imhof H, Glueer C, Adams JE (1999) Imaging of trabecular bone structure in osteoporosis. Eur Radiol 9: 1781–1788

Majumdar S, Genant HK, Grampp S, Newitt DC, Truong VH, Lin JC, Mathur A (1997) Correlation of trabecular bone structure with age, bone mineral density, and osteoporotic status: in vivo studies in the distal radius using high resolution magnetic resonance imaging. J Bone Miner Res 12:111–118

Majumdar S, Link TM, Augat P, Lin JC, Newitt D, Lane NE, Genant HK (1999) Trabecular bone architecture in the distal radius using magnetic resonance imaging in subjects with fractures of the proximal femur. Magnetic Resonance Science Center and Osteoporosis and Arthritis Research Group. Osteoporos Int 10:231–239

Meema HE, Meema S (1972) Comparison of microradioscopic and morphometric findings in the hand bones with densitometric findings in the proximal radius in thyrotoxicosis and in renal osteodystrophy. Invest Radiol 7:88–96

Mosekilde L, Eriksen EF, Charles P (1990) Effects of thyroid hormones on bone and mineral metabolism. Endocrinol Metab Clin North Am 19:35–63

National Osteoporosis Society (2002) The use of quantitative ultrasound in the management of osteoporosis. Position statement of 31 January 2002

Newitt DC, van Rietbergen B, Majumdar S (2002) Processing and analysis of in vivo high-resolution MR images of trabecular bone for longitudinal studies: reproducibility of structural measures and micro-finite element analysis derived mechanical properties. Osteoporos Int 13:278–287

Pacheco EM, Harrison EJ, Ward KA, Lunt M, Adams JE (2002) Detection of osteoporosis by dual X-ray absorptiometry (DXA) of the calcaneus: is the WHO criterion applicable? Calcif Tissue Int 70:475–482

Park EA (1932) The Blackader Lecture on some aspects of rickets. Can Med Assoc J 26:3–15

Parker BR (1981) Hypothyroidism with epiphysial dysgenesis. AJR Am J Roentgenol 136:1030

Picard D, Brown JP, Rosenthall L, Couturier M, Lévesque J, Dumont M, Ste-Marie LG, Tenenhouse A, Dodin S (2004) Ability of peripheral DXA measurement to diagnose osteoporosis as assessed by central DXA measurement. J Clin Densitom 7:111–118

Resnick D (1995a) Acromegaly and gigantism. In: Resnick D (ed) Diagnosis of bone and joint disorders. Saunders, Philadelphia, pp 1971–1992

Resnick D (1995b) Hypopituitarism. In: Resnick D (ed) Diagnosis of bone and joint disorders. Saunders, Philadelphia, pp 1992–1993

Resnick D (1995c) Hyperthyroidism. In: Resnick D (ed) Diagnosis of bone and joint disorders. Saunders, Philadelphia, pp 1995–1999

Resnick D (1995d) Hyperparathyroidism. In: Resnick D (ed) Diagnosis of bone and joint disorder. Saunders, Philadelphia, pp 2012–2036

Resnick D (1995e) Rickets and osteomalacia. In: Resnick D (ed) Diagnosis of bone and joint disorder. Saunders, Philadelphia, pp 1885–1922

Resnick D (1995f) Hypoparathyroidism. In: Resnick D (ed) Diagnosis of bone and joint disorder. Saunders, Philadelphia, pp 2061–2064

Ross PD (1998) Epidemiology of osteoporosis. In: Genant HK G, Jergas M (eds) Bone densitometry and osteoporosis. Springer, Heidelberg, pp 21–42

Rüegsegger P, Elsasser U, Anliker M, Gnehm H, Kind H, Prader A (1976) Quantification of bone mineralization using computed tomography. Radiology 121:93–97

Sartoris D (1971) Acromegaly. In: Sartoris D (ed) Musculoskeletal imaging. Mosby-Year Book, St. Louis, pp 302–303

Sartoris D (1996) Hypothyroidism. In: Sartoris D (ed) Muskuloskeletal imaging. Mosby-Year Book, St. Louis, pp 301–302

Schattauer GmbH (2006) Evidence-Based DVO Guidelines Osteoporosis in Germany; prophylaxis, diagnosis and therapy in postmenopausal women and men over 60 years. Verlag fur medizin und naturwissenschaften, 70174 Stuttgart

Schneider P, Börner W (1991) Peripheral quantitative computed tomography for bone mineral measurement using a new special QCT-scanner. Methodology, normal values, comparison with manifest osteoporosis. Rofo 154:292–299

Schneider P, Reiners C (1998) Peripheral quantitative computed tomography. In: Genant HK, Guglielmi G, Jergas M (eds) Bone densitometry and osteoporosis. Springer, Heidelberg, pp 349–363

Schott AM, Weill-Engerer S, Hans D, Duboeuf F, Delmas PD, Meunier PJ (1995) Ultrasound discriminates patients with hip fracture equally well as dual energy X-ray absorptiometry and independently of bone mineral density. J Bone Miner Res 10:243–249

Seeman E, Delmas PD (2006) Bone quality–the material and structural basis of bone strength and fragility. N Engl J Med 354:2250–2261

Seeman E, Melton LJ 3rd, O'Fallon WM, Riggs BL (1983) Risk factors for spinal osteoporosis in men. Am J Med 75:977–983

Sell CA, Masi JN, Burghardt A, Newitt D, Link TM, Majumdar S (2005) Quantification of trabecular bone structure using magnetic resonance imaging at 3 Tesla–calibration studies using microcomputed tomography as a standard of reference. Calcif Tissue Int 76:355–364

Sornay-Rendu E, Boutry S, Munoz F, Bouxsein ML (2009) Cortical and trabecular architecture are altered in postmenopausal women with fracture. Osteoporos Int 20:1291–1297

Spadaro JA, Werner FW, Brenner RA, Fortino MD, Fay LA, Edwards WT (1994) Cortical and trabecular bone contribute strength to the osteopenic distal radius. J Orthop Res 12:211–218

Stampa B, Kühn B, Liess C, Heller M, Glüer CC (2002) Characterization of the integrity of three-dimensional trabecular bone microstructure by connectivity and shape analysis using high-resolution magnetic resonance imaging in vivo. Top Magn Reson Imaging 13:357–363

Steinbach Hl, Noetzli M (1964) Roentgen appearance of the skeleton in osteomalacia and rickets. Am J Roentgenol Radium Ther Nucl Med 91:955–972

Steinbach H, Gold R, Preger L (1975) Congenital hypothyroidism (cretinoid epiphyseal dysplasia). In: Steinbach H, Gold R, Preger L (eds) Roentgen appearance of the hand in diffuse disease. Year Book Medical Publishers, Chicago, pp 239–241

Sundaram M, Joyce PF, Shields JB, Riaz MA, Sagar S (1979) Terminal phalangeal tufts: earliest site of renal osteodystrophy findings in hemodialysis patients. Am J Roentgenol 133:25–29

Techawiboonwong A, Song HK, Magland JF, Saha PK, Wehrli FW (2005) Implications of pulse sequence in structural imaging of trabecular bone. J Magn Reson Imaging 22:647–655

Theodorou DJ, Theodorou SJ, Resnick D (2001) The hand in endocrine disorders. In: Guglielmi G, Van Kuijk C, Genant HK (eds) Fundamentals of hand and wrist imaging. Springer-Verlag, Heidelberg, p 203

Virtama P (1960) Uneven distribution of bone minerals and covering effect of non-mineralized tissue as reasons for impaired detectability of bone density from roentgenograms. Ann Med Intern Fenn 49:57–65

Vokes TJ, Giger ML, Chinander MR, Karrison TG, Favus MJ, Dixon LB (2006) Radiographic texture analysis of densitometer-generated calcaneus images differentiates postmenopausal women with and without fractures. Osteoporos Int 17:1472–1482

Wehrli FW (2007) Structural and functional assessment of trabecular and cortical bone by micro magnetic resonance imaging. J Magn Reson Imaging 25:390–409

Wehrli FW, Hwang SN, Ma J, Song HK, Ford JC, Haddad JG (1998) Cancellous bone volume and structure in the forearm: noninvasive assessment with MR microimaging and image processing. Radiology 206:347–357

Wehrli F, Gomberg B, Saha P, Song H, Hwang S, Snyder P (2001) Digital topological analysis of in vivo magnetic resonance microimages of trabecular bone reveals structural implications of osteoporosis. J Bone Miner Res 16:1520–1531

Wehrli FW, Saha PK, Gomberg BR, Song HK, Snyder PJ, Benito M, Wright A, Weening R (2002) Role of magnetic resonance for assessing structure and function of trabecular bone. Top Magn Reson Imaging 13:335–355

Wüster C, Albanese C, De Aloysio D, Duboeuf F, Gambacciani M, Gonnelli S, Glüer CC, Hans D, Joly J, Reginster JY, De Terlizzi F, Cadossi R (2000) Phalangeal osteosonogrammetry study: age-related changes, diagnostic sensitivity, and discrimination power. The Phalangeal Osteosonogrammetry Study Group. J Bone Miner Res 15: 1603–1614